Sensors & Transducers, Vol. 237, Issue 9-10, September-October 2019, pp. 122-128

Sensors & Transducers
Published by IFSA Publishing, S. L., 2019
http://www.sensorsportal.com

Negative Ion Instrumentation for Detection of the Electron Affinity of Astatine

Lars E. Bengtsson
University of Gothenburg, Kemivägen 9, 412 96 Gothenburg, Sweden
Tel.: +4631 786 9128
E-mail: lars.bengtsson@physics.gu.se

Received: 30 August 2019 /Accepted: 27 September 2019 /Published: 30 November 2019

Abstract: For the purpose of measuring the electron affinity of Astatine, a versatile tool for ion beam line up is proposed. Apertures in the ion optics are used to guide the beam and traditionally the current is measured on the apertures in order to detect the presence of an ion beam. By slitting the aperture into four separate pieces, the aperture current can also be used to determine the direction of the misalignment and the size of the ion beam diameter. A 4-channel pico ammeter with optical LED indication of the ion beam position is suggested in an analog/digital hybrid design. The design utilizes two charge/current-to-digital chips in a microcontroller design. This work is an important contribution to an ongoing project with the objective to determine the electron affinity of Astatine which is a potential α-radiation agent in radioimmunotherapy.

Keywords: Ion optics, Astatine, Pico ammeter, α-radiation, Radioimmunotherapy, Microcontroller.

1. Introduction

1.1. Background

Radiation therapy is one of the most common treatments for cancer; cancer cells are destroyed by ionizing radiation. However, ionizing radiation may also cause damage to healthy cells and in any radiation therapy it is paramount that the radiation is focused on the cancer cells and avoid non-cancerous cells as much as possible. For example, different radiation angles can be applied in order to minimize the radiation exposure of healthy cells.

Ionizing radiation comes in three different shapes; α-radiation, β-radiation and γ-radiation. α-radiation is basically helium nuclei and the advantage of using α-radiation in cancer therapy is that they cause a lot of damage to the cancer cells due their large impact force; once they penetrate the cell membrane, they shatter the DNA molecule. The disadvantage is that they have a very short range; due to their large size, they interact with surrounding particles and will only travel a few centimeters in air. In order to be used in cancer therapy, they must be injected into the body (brachy therapy) and they are likely to cause as much damage to health tissue as they do to cancer cells.

β-radiation consists of electrons. They are smaller than α-particles and therefore they have a longer range; they can penetrate human skin down to approximately 1 cm. Hence, if tumors are deeper than 1 cm, the β-radiator must also be injected into the body (with similar consequences as α-particles). Also, since electrons are lighter than helium nuclei, a higher radiation dose is required compared to α-radiation.

γ-radiation is high-energetic electromagnetic radiation which easily penetrates the human body and destroys cancer cells. However, their extended range is also likely to cause a lot of "collateral" damage to healthy cells and might actually turn healthy cells into cancer cells.

With this background, it should be obvious that a perfect radiotherapy should consist of an α-radiator that is applied in close proximity of the cancer cell; only the cancer cell would be radiated. In 1975, researchers were able to produce antibodies that only attached to cancer cells (monoclonal) [1] and by engineering the antibody to act as a vehicle for a radioactive agent, α-radiators can be delivered directly to the cancer cells, causing minimal damage to surrounding health cells ("radioimmunotherapy").

Apart from being an α-radiator, the perfect radiation agent should have a suitable half-lifetime (should live long enough to reach the target cell but should decay fast enough after the elimination of the cancerous cell) and it should decay into elements that are non-toxic to the human body; the daughter atoms detach from the antibody and may spread to other vital organs. Bismuth (213) and Actinium (225) have been used [2-3] but Bismuth-213 has a half-lifetime of only 46 minutes and Actinium-225 is very hard (and expensive) to produce. For that reason, other α-radiation agents for radioimmunotherapy are constantly investigated. One element that has been identified as a suitable agent for this purpose is Astatine-211. It has a half-lifetime of 7.2 hours and its decay chain is more beneficial to the patient compared to Bismuth and Actinium [4].

In order to attach Astatine-211 to a cancer cell-targeting antibody, its chemical properties must be fully understood, and the primary purpose of this work was to contribute to this understanding by measuring the electron affinity of negative ions of Astatine-211. However, Astatine is one of the rarest elements in the Earth's crust and must be synthetically produced (that is the reason why its chemical properties have not been studied). For commercial production, Astatine can be produced by bombarding Bismuth with α-particles, but this work will take place at the ISOLDE facility at CERN where a beam of negative Astatine ions is produced in the particle accelerator.

1.2. Ion Optics

The electron affinity of a negative ion is the binding energy of the extra electron and is measured by photon detachment; the ion is radiated with light from a tunable laser and when the laser wavelength is short enough, the electron is detached, and the ion is neutralized. While the negatively charged ions are deviated by magnetic fields, the neutral atoms are unaffected and can be individually detected by a multi-channel plate detector. In order to compensate for Doppler effects, ions are irradiated with two laser beams from opposite directions and since the density of the Astatine ions is quite small, the laser-ion interaction region must be quite long (> 1 meter). Hence, the ion beam trajectory, from the particle accelerator source to the final detector is very long and needs to be controlled by multiple deflector plates and Einzel lenses. The process of lining up the ion beam is typically a long-suffering and tedious job since it requires guiding the ions through a long range of ion optics [5]. Fig. 1 illustrates an example of the kind of ion optics that is frequently used.

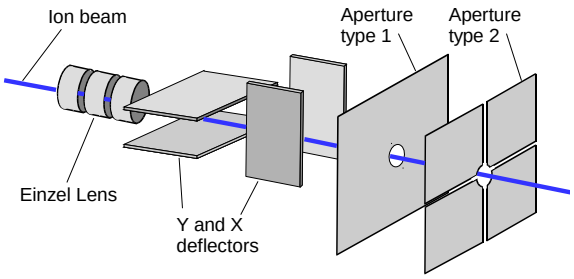

Fig. 1. Ion beam optics example.

Einzel lenses are used to focus the beam and deflector plates are used to control the beam trajectory in the X and Y directions. Apertures are used to narrow the beam diameter but are also useful indicators of the beam quality and direction. Ideally, the current registered on any aperture plate should be zero. The apertures' current is a crucial parameter to monitor during ion beam line-up.

Ion beam currents are of the order of nano amps at best and sub-pico amps at worst and hence this requires sensitive ammeters with careful design layouts.

Commercial sub-pico ammeters are very expensive; a desktop instrument could cost as much as $5,000 [6] and in order to line up an ion beam, multiple ammeters are required. For these reasons, a versatile, non-expensive multi-channel ammeter with pico ampere capability has been requested.

There are in principle two basic ammeter circuits; the shunt ammeter and the feedback ammeter [7]. This work is based on the DDC112 chip from Texas Instruments [8] which contains two capacitive-feedback ammeters [9]. The instrument should primarily be used to line up the ion beam through the ion optics to the target. Hence the accuracy, resolution and absolute values are not crucial, but the tool should be able to indicate ion currents of the order of 1 pA or less.

1.3. Problem Description

A typical aperture plate has a circular hole in the center (left side of Fig. 2). This aperture design will narrow the ion beam and by tapping off its current an indication of the misalignment is achieved but it will not reveal the direction of the misalignment. For that reason, the aperture is sliced into four separate pieces, see Fig. 2, right side.

By measuring the current separately on all four aperture plates, it is possible to determine the direction of the misalignment and also draw some conclusions about the beam quality; a large current on one plate

indicates a misalignment in that direction and a current on all plates indicates a wide beam. The disadvantage is that in order for the quad-aperture to be really useful, it requires that the four currents are measured simultaneously; an inexpensive four-channel pico ammeter is required.

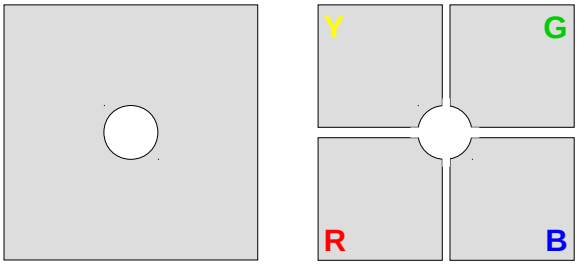

Fig. 2. Ion optics apertures.

1.4. Proposed Solution

An analog/digital hybrid 4-channel picoamp tool will be designed. Each one of the four aperture plates will be color-coded (Yellow, Green, Red and Blue). Four pico ammeters will be implemented on the same PCB based on two DDC112 chips. The digitized current is transferred to a microcontroller via a synchronous serial interface (SPI compatible) and can optionally be relayed to a host computer, but this is primarily a stand-alone desktop instrument intended as an ion beam guiding tool. The instrument panel will have four sets of four colored LEDs as illustrated in Fig. 3.

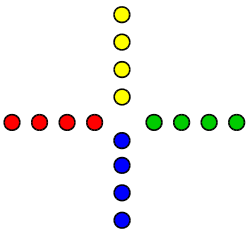

Fig. 3. The instrument panel has four arrays of LEDs.

Each colored LED array corresponds to the ion current on the corresponding aperture plate. This will offer a convenient optical indication of the ion beam's (mis)alignment. Some examples are illustrated in Fig. 4 through 6. Notice that a high degree of activity on the LEDs indicates a misaligned or broad ion beam and a low activity (or no activity) indicates a clean passage through the aperture.

The prototype version of this versatile instrument will have a single range only, but the next version will have a front panel knob for the selection of different ranges (20 pA, 50 pA, 100 pA and 1000 pA). Also, an LCD display will be added in order to display the exact current values on each channel.

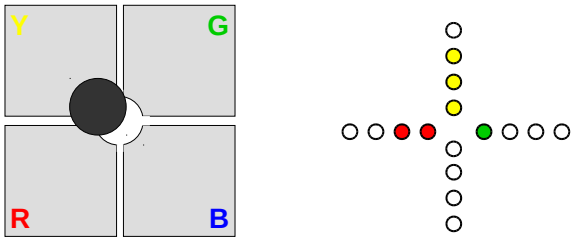

Fig. 4. Ion beam too broad and too far to the upper left.

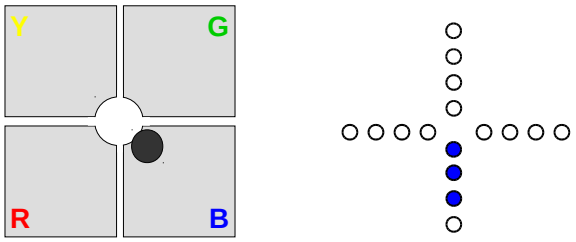

Fig. 5. Ion beam too far to the lower right (but size is probably ok).

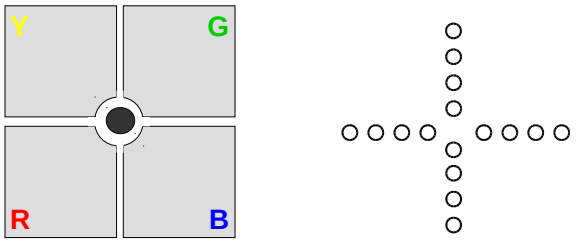

Fig. 6. No LEDs turned on indicates that the ion beam passes the aperture in the center of the Z direction (beam passes through unobstructed).

2. Design

2.1. Hardware

At the core of the design are two DDC112 chips from Texas Instruments [8]. This 28-pin SO-chip has two charge input channels (sharing the same 20-bit ΣΔ ADC) and each channel comprises two classical analog charge integrators; while one is being digitized, the other one is being charged. Hence, the input charge/current is seamlessly monitored. The range depends on the feedback capacitor and the integration time. Internal feedback capacitors are available but external capacitors can also be used. The integration time is provided by the user by toggling the CONV pin. Fig. 7 illustrates the pin layout and Fig. 8 is a (simplified) model of input channel 1.

The switches in Fig. 8 alternately charges/ discharges the feedback capacitors and forward the integrators' outputs to the ADC for digitalization. The switches are controlled by an internal synchronous state machine in order to charge/discharge the capacitors and to relay the two integrator outputs to the ADC alternately. Fig. 9 illustrates the timing diagram;

input integrators A (on both channels) are integrated simultaneously while integrators B are being digitized by the AD converter. The signal indicates when both channels have been digitized and data is stored in a 40-bit shift register.

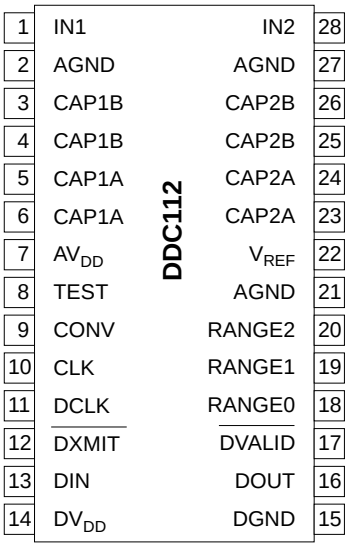

Fig. 7. Current-to-digital converter (DDC112).

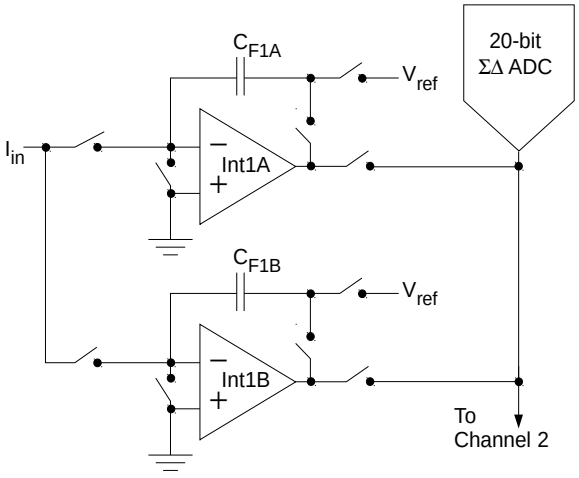

Fig. 8. Charge-input integrator.

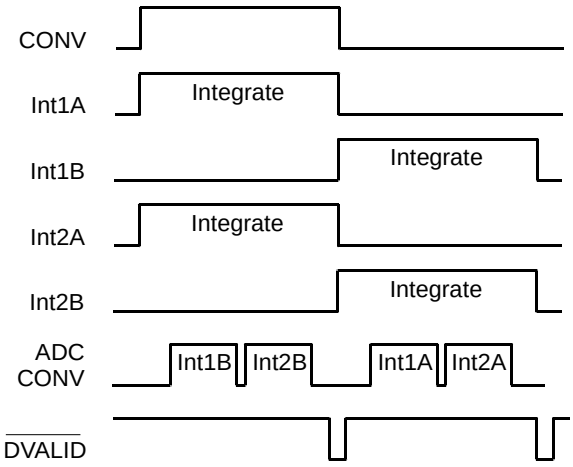

Fig. 9. Integration timing diagram.

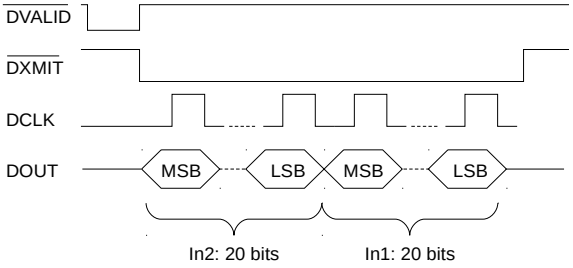

Fig. 10. Timing diagram of data retrieval.

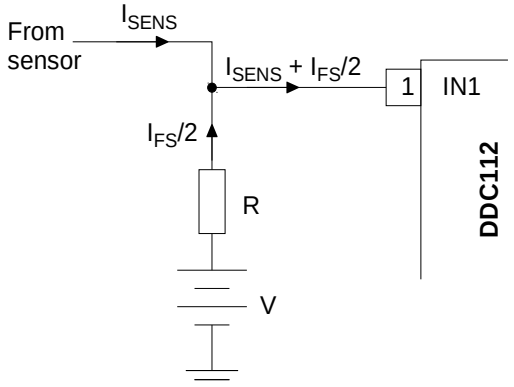

Fig. 11. Bipolar input.

The user retrieves data through the synchronous serial interface (pins DCLK and DOUT). This is illustrated in Fig. 10 [10].

Transmission is initiated by the user setting the signal low and data is shifted out on the DOUT pin synchronous to the rising edges on the DCLK pin. Notice in Fig. 10 that the signal is automatically reset when transmission is initiated.

The primary concern in this design is to detect negative ion currents or electrons. However, sometimes positive ion experiments are conducted and for that reason the instrument needs to be able to detect both positive and negative currents. The DDC112 chip can easily be converted to a bipolar ammeter by adding an offset current to the input, see Fig. 11 [11].

The ADC in the DDC112 chip has a resolution of 20 bits; if the input current equals the full-scale current (I_{FS}), the ADC output will be 0xFFFFF (2^{20} -1). *V* and *R* in Fig. 11 will produce an offset current *V*/*R* and this current is added to the sensor current. In order to make the instrument bipolar, *V* and *R* are dimensioned so that $V/R = I_{FS}/2$.

The two currents from the sensor and the offset branch are added in the junction and the sum of the two currents are fed to the DDC112 chip. The consequence of that is that when the sensor input current $I_{SENS} = -I_{FS}/2$, the input current to the DDC112 chip is zero. Table 1 illustrates the consequence of the offset current. From Table 1 it is obvious that the instrument is now bipolar.

Table 1. ADC output vs sensor current.

I_{SENS}	Input current	ADC output
$I_{FS}/2$	I_{FS}	0xFFFFF
0	$I_{FS}/2$	0x7FFFF
$-I_{FS}/2$	0	0x00000

2.2. Current Range Calculations

The aim is to create a bipolar instrument with a full-scale range of ±50 nA. Due to the bipolar circuitry in Fig. 11, this means that the maximum input current to the DDC112 chip is 100 nA. With a 20-bit ADC resolution, the current resolution will be

$$\frac{100\text{ nA}}{2^{20}} = 95\text{ fA}, \quad (1)$$

which is less than the expected noise level (≈ 2 pA).

If we choose internal feedback capacitors 87.5 pF, the required integration time for a full-scale range of 100 nA is [8]

$$T_{int} = \frac{0.96 \times V_{ref}}{I_{FS}} \times C_F \quad (2)$$

$$T_{int} = \frac{0.96 \times 5.0}{100 \times 10^{-9}} \times 87.5 \times 10^{-12} = 4.2\text{ ms}$$

This time is important not only for the integration; from Fig. 10 we can see that in order to retrieve the old data before the next data is digitized, 40 clock pulses must be generated during this time. Hence, the minimum clock rate on the synchronous serial interface is

$$f_{DCLK,min} = \frac{40}{0.0042} = 9523\text{ Hz}$$

In order to allow for some overhead, the DCLK clock rate will be at least 20 kHz.

2.3. The Microcontroller Design

The two DDC112 charge integrating chips are connected to an 8-bit PIC16F1779 microcontroller [12] as described in Fig. 12.

Notice in Fig. 12 how the two DDC112 chips have been cascaded; the data from the first one will be shifted through the second chip. The data is transferred to the microcontroller via a synchronous serial interface and from Fig. 10 it is clear that signals DXMIT, DCLK and DOUT complies with a standard SPI interface (or a clocked USART interface).

In this first prototype, data will be translated to different diode levels, four on each collimator plate, and the high-resolution DDC112 chip may appear to be an overkill. However, the use of the DDC112 chips makes the design easier (compared to using op amps) and since they make the absolute current values available (high-resolution), it would be easy to modify the design to either display them locally on an LCD or transfer them to a host computer. Also, a front panel knob will be added to allow for four different full-scale ranges (20 pA, 50 pA, 100 pA and 1000 pA).

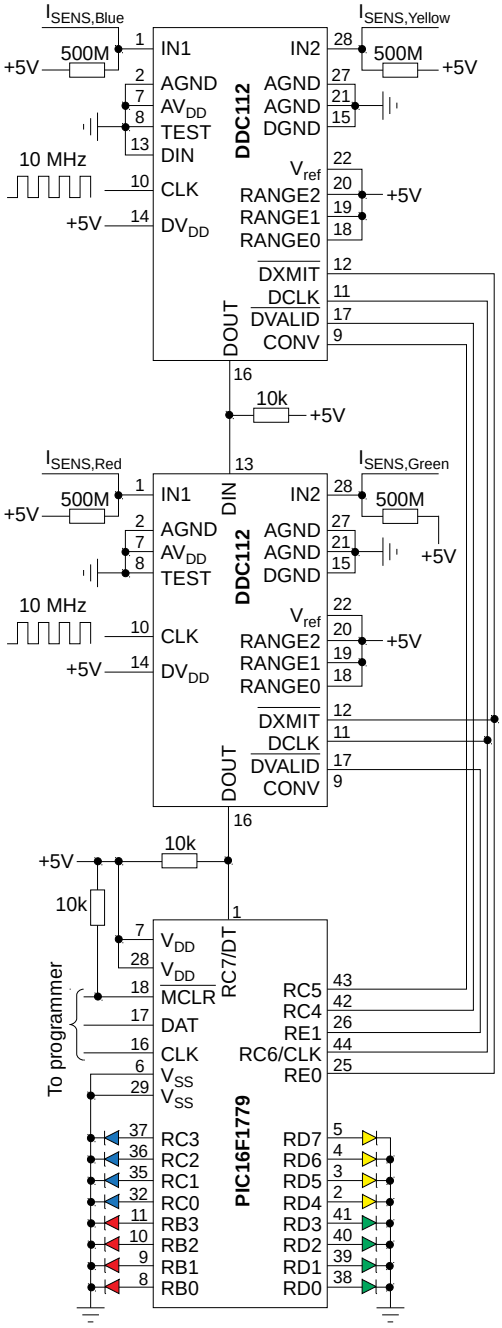

Fig. 12. 4-channel pico ampermeter.

In all sub-nano current designs, it is important to protect the inputs from stray wire capacitances. In order to facilitate an expedient PCB layout for this purpose, the two analog inputs are located at the top of the DDC112 chip and the next two pins are analog ground [7]. This makes it easy to surround the analog inputs with a shielding copper layer on the pcb [8] as illustrated in Fig. 13.

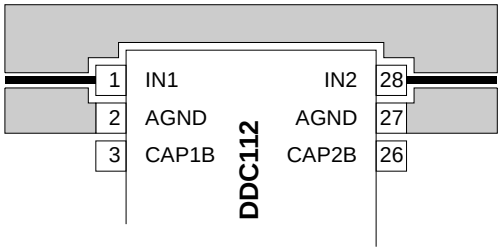

Fig. 13. Input signals are protected from stray capacitances.

3. Related/previous Work

The DDC112 chip is a common solution to low-current/low-charge problems. It has been used in precise current integrators in scanning tunneling microscopes and atomic force microscopy [13], measuring sub-picoamp currents from Faraday cup detectors [14], ion beam monitoring in deep proton lithography [15] and as photometric analyzers in optical telescopes [16]. The idea explored in this work, where an ion optics collimator plate is split into four symmetric pieces, was first suggested by Snowden and Barber [17] but their application was for microamp currents and used shunting resistors in a bridge to detect the current. The main difference of this work is that it utilizes the versatile DDC112 chip (based on charged integration), it has the option to transfer absolute current values to a host computer and offers the convenient visual indication of the beam position facilitated by the front panel LEDs.

Astatine is a halogen element, located right below Iodine in the periodic table, and its chemical properties are expected to be close to that of Iodine. The electron affinity of iodine has previously been measured to 3.059 038(10) eV [18]. Since the Astatine has one more electron orbit than Iodine, the extra electron in the negative Astatine ion will be further away from the nucleus and the electrostatic attraction force will be smaller; the electron affinity of Astatine is expected to be less than that of Iodine. This is also in accordance with theoretical predictions which range from 2.30 to 2.90 eV [19-21].

Different tumors have different antigens and therefore the antibody-antigen biding differs for different kinds of tumors; the antibody must be designed specifically for the active tumor's antigens and the chemical bonding between the radiation agent and the antibody must be strong enough, so that it isn't released before it has reached the cancer cell; once the antibody has docked with the antigens, the antibody is absorbed by the cell and the radiation agent can destroy the DNA protein in the cell nucleus. The antibody with the radiation agent is illustrated in Fig. 14, and Fig. 15 illustrates the antibody-antigen bonding. Fig. 16 illustrates how the cell nucleus (holding the DNA molecule) is exposed to α-radiation once the antibody has penetrated the cell surface.

This method was first practiced in 1958 when it was used in leukemia therapy [22]. However, in "solid" tumors, the penetration rate is poor and for that reason non-internalizing antibody-drugs are being researched [23-24].

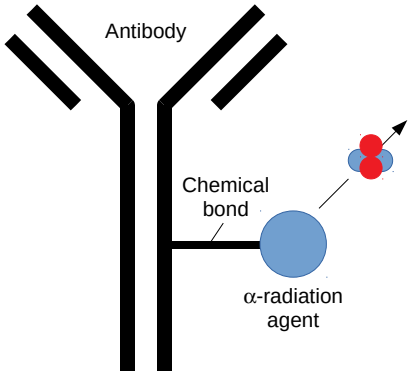

Fig. 14. Antibody as a vehicle for anti-cancer drug.

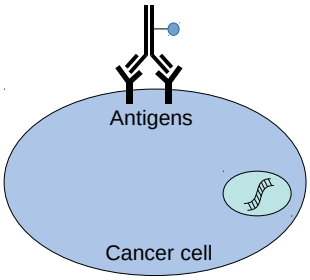

Fig. 15. Antibodies are designed to attach only to carcinogenic cells (of a specific kind).

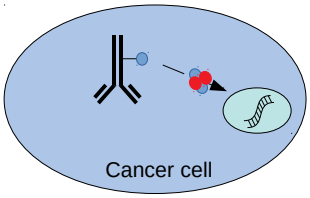

Fig. 16. Antibodies are designed to attach only to carcinogenic cells (of a specific kind).

4. Conclusions

A microcontroller based, 4-channel pico ammeter is being developed for the purpose of facilitating convenient line up of ion beams in particle physics experiments at the GANDALPH setup at the CERN-ISOLDE facility. Instead of devolving to discrete feedback opamp solutions, two, 2-channel charge integrating chips are employed. This solution is less expensive, more robust, simplifies PCB layout and facilitates a digital interface for retrieving the absolute current value.

A prototype will be tested in October 2019 and beta testing will be performed in the Atomic Physics Laboratories in Gothenburg during the fall before the instrument is shipped to the CERN ISOLDE facility later this year.

Acknowledgements

The preliminary version of this work was first presented at the *5th International Conference on Sensors and Electronic Instrumentation Advances 2019* [25]. The author has no other conflicts of interest to report.

References

[1]. G. Kohler, C. Milstein, Continuous cultures of fused secreting antibody of predefined destiny, *Nature,* Vol. 256, 1975, pp. 495-497.

[2]. M. McDevitt, G. Sgouros, R. D. Finn, J. L. Humm, J. Juric, S. Larson, D. Scheinberg, Radioimmunotherapy with alpha-emitting nuclides, *European Journal of Nuclear Medicine,* Vol. 25, Issue 9, 1998, pp. 1341-1351.

[3]. J. Juric, Clinical Studies with Bismuth-213 and Actinium-225 for Hematologic Malignancies, *Current Radiopharmaceuticals,* Vol. 11, Issue 3, 2018, pp. 192-199.

[4]. M. Zalutsky, M. Pruszynski, Astatine-211: Production and Availability, *Current Radiopharmaceuticals,* Vol. 4, Issue 3, 2011, pp. 177-185.

[5]. D. A. Skoog, J. J. Leary, Principle of Instrumental Analysis, 4th ed., *Saunders College Publishing*, Orlando, Florida, 1992, pp. 429-432.

[6]. Tektronix Inc., Keithley Series 6400 Picoammeters, *Tektronix, Inc*., 19 March 2018. [Online]. Available: https://www.tek.com/keithley-low-level-sensitive-and-specialty-instruments/keithley-series-6400-picoammeters. [Accessed 19 March 2018].

[7]. Keithley Instruments, Inc., Low Level Measurments Handbook, 6th ed., *Keithley Instruments, Inc.*, Cleveland, Ohio, 2004.

[8]. Texas Instruments, Burr-Brown, DDC112: Dual Current Input 20-bit Analog-to-Digital Converter, *Texas Instruments*, 2004.

[9]. A. A. Mortuza, F. Pervez, K. Hossain, S. K. Sen, N. H. Mia, M. K. Basher, S. Alam, Pico-current Measurement Challenges and Remedies: A Review, *Universal Journal of Engineering Science,* Vol. 5, Issue 4, 2017, pp. 57-63.

[10]. J. Todsen, Retrieving data from the DDC112, *Burr-Brown Corporation*, Tucson, Arizona, 1998.

[11]. J. Todsen, Creating a bipolar input range for the DDC112, *Burr-Brown Corporation*, Tucson, Arizona, 1999.

[12]. PIC16(L)F1777/8/9, *Microchip Technology Inc*., Tucson, Arizona, 2015-2016.

[13]. K. Raczkowski, T. Piasecki, M. Rudek, T. Gotszalk, Design and evaluation of precise current integrator for scanning probe microscopy, *Measurement Science and Technology,* Vol. 28, Issue 3, 2017, pp. 1-9.

[14]. S. Agosteo, E. Borsato, F. Corso, A. Fazzi, F. Gonella, M. Intrioni, I. Lippi, M. Lorenzoli, L. Modense, F. Montecassiano, M. Pegoraro, A. Pola, V. Varoli, P. Zotto, Performance of a proton irradiation chamber, *Nuclear Instruments and Methods in Physics Research Section A: Accelerator, Spectrometers, Detectors and Associated Equipment,* Vol. 664, Issue 1, 2012, pp. 193-202.

[15]. P. Vynck, B. Volckaerts, M. Vervaeke, H. Ottevare, P. Tuteleers, L. Cosentino, P. Fincchiaro, A. Pappalardo, A. Hermanne, H. Thienpont, Beam monitoring enhances deep proton lithography: towards high-quality micro-optical components, in *Proceedings of the Symposium IEEE/LEOS Benelux Chapter*, Amsterdam, 2002.

[16]. R. S. Romaniuk, Space and High Energy Experiments Advanced Electronic Systems 2012, *Intternational Journal of Electronics and Telecommunications,* Vol. 58, Issue 4, 2012, pp. 441-462.

[17]. K. Snowdon, C. Barber, Simple accelerator beam position monitor, *Journal Physics E: Scientific Instruments,* Vol. 12, Issue 10, 1979, p. 923.

[18]. D. Hanstorp, M. Gustafsson, Determination of the electron affinity of iodine, *Journal of Physics B: Atomic, Molecular and Optical Physics,* Vol. 25, Issue 8, 1992, pp. 1773-1783.

[19]. A. Mitin, C. van Wullen, Two-component relativistic density-functional calculations of the dimers of the halogens from bromine through element 117 using effective core potential and all-electron methods, *Journal of Chemical Physics,* Vol. 124, 2006, 064305.

[20]. H. Hotop, W. Lineberger, Binding Energies in Atomic Negative Ions: II, *Journal of Physical and Chemical Reference Data,* Vol. 14, Issue 3, 1985, pp. 731-750.

[21]. S. Hughes, U. Kaldor, The Fock-space coupled-cluster method: Electron affinities of the five halogen elements with consideration of triple excitations, *Journal of Chemical Physics,* Vol. 99, Issue 9, 1993, pp. 6773-6776.

[22]. G. Mathé, T. Loc and J. Bernard, Effet sur la leucemie 1210 de la souris d'un combinaison par diazotation d'A-methopterin et de γ-globulines de hamsters porteurs de cette leucemie par heterograffe, *Comptes Rendus de l'Académie des Sciences,* Vol. 216, 1958, pp. 1626-1628.

[23]. Joubert N., Denevault-Sabourin C., Bryden F., Viaud-Massuard M.-C., Towards antibody-drug conjugates and prodrug strategies with extracellular stimuli-responsive drug delivery in the tumor microenvironment for cancer therapy, *European Journal of Medicinal Chemistry*, Vol. 142, 2017, pp. 393-415.

[24]. A. D. Corso, R. Gébleux, P. Murer, A. Soltermann, D. Neri, A non-internalizing antibody-drug conjugate based on an anthracycline payload displays potent therapeutic activity in vivo, *Journal of Controlled Release,* Vol. 264, 2017, pp. 211-218.

[25]. L. Bengtsson, An Ion Beam Guidance Control Tool Proposal, in *Proceedings of the 5th International Conference on Sensors and Electronic Instrumentation Advances (SEIA' 2019)*, Teneriffe (Canary Islands), Spain, 25-27 September 2019, pp. 28-32.